NASA Contractor Report 194899

ICASE Report No. 94-21

ICASE

THE VELOCITY FIELD CREATED BY A SHALLOW BUMP IN A BOUNDARY LAYER

Michael Gaster
Chester E. Grosch
Thomas L. Jackson

Contract NAS1-19480
April 1994

Institute for Computer Applications in Science and Engineering
NASA Langley Research Center
Hampton, VA 23681-0001

Operated by Universities Space Research Association

ICASE Fluid Mechanics

Due to increasing research being conducted at ICASE in the field of fluid mechanics, future ICASE reports in this area of research will be printed with a green cover. Applied and numerical mathematics reports will have the familiar blue cover, while computer science reports will have yellow covers. In all other aspects the reports will remain the same; in particular, they will continue to be submitted to the appropriate journals or conferences for formal publication.

THE VELOCITY FIELD CREATED BY A SHALLOW BUMP IN A BOUNDARY LAYER

M. Gaster

University of Cambridge
Cambridge CB2 1PZ England

C. E. Grosch

Old Dominion University
Norfolk, Virginia 23529 USA

T. L. Jackson

Institute for Computer Applications
in Science and Engineering
NASA Langley Research Center
Hampton, Virginia 23681 USA

ABSTRACT

We report the results of measurements of the disturbance velocity field generated in a boundary layer by a shallow three-dimensional bump oscillating at a very low frequency on the surface of a flat plate. Profiles of the mean velocity, the disturbance velocity at the fundamental frequency and at the first harmonic are presented. These profiles were measured both upstream and downstream of the oscillating bump. Measurements of the disturbance velocity were also made at various spanwise and downstream locations at a fixed distance from the boundary of one displacement thickness. Finally, the spanwise spectrum of the disturbances at three locations downstream of the bump are presented.

The authors were supported, in part, by NATO Collaborative Research Grant 900164. CEG and TLJ were also supported, in part, by the National Aeronautics and Space Administration under NASA Contract NAS1-19480 while in residence at the Institute for Computer Applications in Science and Engineering, NASA Langley Research Center, Hampton, VA 23681-0001.

1. Introduction.

This project was started to answer questions that arose during discussions about the disturbance field created by a localised boundary perturbation of a boundary layer flow. At that time two of the authors (CEG and TLJ) were working on the eigenmodes of the boundary layer equations, while the other (MG) was using the Orr-Sommerfeld approach to tackle boundary value problems in parallel flows. Whereas the first approach appears to be the most appropriate because it can account for boundary layer growth, it was argued that the Orr-Sommerfeld model retained the essential elliptic nature of the Navier-Stokes equation. We decided to find out what the solution looked like by doing this experiment. It transpired that the measurements do not seem to be consistent with either model, but they maybe of interest to others. The disturbance flow field in a boundary layer created by a shallow bump (whether of fixed height or oscillating) on the boundary has been studied using triple deck theory by a number of authors; for example, Smith (1982) and references contained therein and Duck and Burggraf (1986). Typically these authors report the wall pressure and shear stress distributions caused by these disturbances. As far as we know there are no predictions or experimental measurements of the velocity field created such a static bump or one oscillating at a very low frequency. G. I. Taylor (1939), in a very important paper presented to IUTAM in 1938, discussed transition of a boundary layer on a flat plate. At that time the stability theories of Tollmien and Schlichting and others were not universally accepted as no such waves had been observed during the transition process. In fact the experiments carried out in Cambridge had shown distributions in fluctuations across the layer of a somewhat different form more consistent with a heaving motion of the boundary layer rather than of an eigenmode of the instability system. In more recent times Klebanoff also observed these modes and he made some measurements showing that they were essentially three-dimensional. This type of low frequency motions is now commonly called a Klebanoff mode. A proper mathematical account of these disturbances has not yet appeared. It is thought that the experimental measurements reported here contribute to our knowledge of such modes.

We have carried out an experiment to measure the disturbance flow field in a flat plate boundary layer caused by a shallow bump on the surface of a plate. At low frequency the boundary conditions that have to be imposed on the x-axis in order to represent an oscillating bump are a streamwise velocity perturbation related to the mean shear and the bump height together with the normal velocity of the bump. If the frequency of oscillation is low it turns out that the normal velocity component of this boundary condition is small, as will be shown in the next section. For the parameter values used here the motion can be considered to be essentially quasi-static. It is convenient to introduce a periodic perturbation for purely experimental reasons. A static distortion of the flow field would have been almost impossible to measure, especially with hot-wire anemometry. The small periodic signals obtained from the anemometer system were ensemble averaged over many cycles of oscillation, enhancing the signal-to-noise ratio considerably.

In the next section we consider the boundary conditions for oscillating and stationary bumps. Section 3 is a description of the experimental conditions and results are presented in section 4. Finally, the summary is presented in Section 5.

2. Boundary Conditions For Oscillating And Stationary Bumps.

Let $\vec{u}$ be the velocity of the fluid and $\vec{V}$ be the velocity of the boundary. The amplitude of the bump is ε (assumed to be small) and its shape is $h(x,z)$ and has compact support. The boundary is the surface, S, given by

$$y = \varepsilon h(x,z)\, e^{-i\omega t}, \tag{1}$$

where $h(x,z)$ has been normalized such that its maximum is one. The boundary condition is that, on S,

$$\vec{u} = \vec{V}, \tag{2}$$

with

$$\vec{V} = \hat{i}\,\frac{dx}{dt} + \hat{j}\,\frac{dy}{dt} + \hat{k}\,\frac{dz}{dt} = \hat{i}\,[0] + \hat{j}\,\varepsilon[-i\,\omega h(x,z)\, e^{-i\omega t}] + \hat{k}\,[0]. \tag{3}$$

Expanding the velocity as

$$\vec{u} = \vec{u}_0 + \varepsilon\vec{u}_1 + \varepsilon^2\vec{u}_2 + \ldots \tag{4}$$

so that on the boundary S we have

$$\begin{aligned}&\vec{u}_0(x, \varepsilon h(x,z)\, e^{-i\omega t}, z) + \varepsilon\vec{u}_1(x, \varepsilon h(x,z)\, e^{-i\omega t}, z) + \\ &\varepsilon^2\vec{u}_2(x, \varepsilon h(x,z)\, e^{-i\omega t}, z) + \quad \ldots \quad = \hat{j}\,\varepsilon[-i\,\omega h(x,z)\, e^{-i\omega t}].\end{aligned} \tag{5}$$

Expand each of the $\vec{u}_n$ in a Taylor series about $y = 0$ and substitute into equation (5). Equating successive powers of ε to zero yields the boundary conditions for the $\vec{u}_n$.

Assuming that the mean flow is Blasius (or Falkner-Skan) gives,

$$\vec{u}_0 = (u_0(\eta), v_0(x,\eta), 0), \tag{6}$$

with $\eta = y/\sqrt{2x}$ and $u_0 \equiv F'(\eta)$. This yields at $O(1)$,

$$u_0(0) = 0, \qquad v_0(x,0) = 0. \tag{7}$$

As expected the $O(1)$ terms are unchanged by the presence of a bump. For succeeding orders we set

$$\vec{u}_n = (u_n(x,\eta,z), v_n(x,\eta,z), w_n(x,\eta,z))\, e^{-i n \omega t}, \qquad n = 1,2,\ldots \tag{8}$$

so that at $O(\varepsilon)$,

$$u_1(x,0,z) = -h(x,z) F''(0)/\sqrt{2x}, \qquad v_1(x,0,z) = -i\,\omega h(x,z), \qquad w_1(x,0,z) = 0. \tag{9}$$

From these boundary conditions one sees that at the boundary the lowest order disturbance velocity field is 180^o out of phase with the motion of the bump and is confined to the region of the bump. The component in the mean flow streamwise direction, u_1, is proportional to the shear stress of the undisturbed mean flow at the boundary and to the local height of the bump. The factor of $1/\sqrt{2x}$ arises from the effective decrease in the height of the bump relative to the thickness of the boundary layer as the location of the bump is moved downstream (h is normalized so that its maximum is one). At very low frequency ($\omega \to 0$) only u_1 is nonzero. The bump oscillating at low frequency generates a quasi-steady flow field. It is straightforward to calculate the boundary condition for $\vec{u}_2$ by equating the terms at $O(\varepsilon^2)$. It is seen that $\vec{u}_2$ has double the frequency and is proportional to h^2. Thus, even if the flow disturbance is small enough for linearization to be valid harmonics of the fundamental forcing frequency will be present because of the nonlinear boundary conditions.

3. Experimental Conditions.

The experiments were carried out in a low turbulence wind tunnel in the Department of Engineering, University of Cambridge. The tunnel has a working section which is 3.50 meters long and has a 0.91 meter by 0.91 meter cross section. The speed range of the tunnel is 0 to 50 meters/second, but all of the experiments reported here were carried out at a speed of 18.10 meters/second. The measured free-stream turbulence level in the tunnel at this speed in a frequency range 4Hz to 10Khz is 0.01%.

The plate was mounted vertically in the center of the tunnel. The plate was made from 3/8 inch thick aluminium alloy of a free machining quality in order to avoid distortion. The leading edge was machined on the plate to form a super ellipse of degree 3 with a ratio of major-to-minor axis of 12. A flap with a small tab at the trailing edge of the plate was provided tc control the pressure gradient on the plate.

The bump was constructed from a circular Silicon rubber diaphragm 20 mm in diameter mounted in a disk insert of 200 mm diameter. The disk insert was flush mounted in the plate on the center line with the diaphragm 400 rnm from the leading edge of the plate. In Figure 1 the circle labeled S shows the location of the bump; but note that this sketch is not to scale. The motion of the diaphragm was controlled by an electro-

mechanical vibrator through a coupling rod on the reverse side of the plate. The vibrator was mounted on the side wall of the tunnel. It was very difficult to measure the amplitude of the driver motion; we estimate that it was 0.12 mm ± 50%. The diaphragm was moulded so that most of the motion occurred only over the central portion of roughly 10-15 mm diameters. The diaphragm was driven at a frequency of 2 Hz in all experiments.

The wind tunnel is equipped with a computer controlled three-dimensional traverse for the hot-wire probe together with the usual A/D converters to obtain hot-wire signals and a D/A to drive the diaphragm synchronously. This enabled much of the experiment to be controlled by a computer. Programs were written to acquire various forms of record without intervention, enabling us to use the nights to obtain data requiring the most amount of averaging.

With the flow speed of 18.10 meters/second and air temperature of 20^o C the unit Reynolds number $U_\infty / \nu = 1.21 x\ 10^4$ 1/cm. At the location of the bump, 400 mm from the leading edge, $Re_x = 4.84 x\ 10^5$. The air temperature in the tunnel was a nominal 20^o C. However during the period of the experiment the air temperature changed by a few degrees C so that the unit Reynolds number varied by ± 3%. The flap and tab on the trailing edge of the plate were adjusted to give a nearly uniform pressure distribution on the plate so that the mean flow velocity profiles in the boundary layer conformed closely to the theoretical Blasius solution. The undisturbed boundary layer thickness at the location of the bump was $\delta = 2.88$ mm and the corresponding displacement thickness $\delta^* = 0.99$ mm. The boundary layer Reynolds nurnbers, also at the location of the bump, were $Re_\delta = 3480$ and $Re_{\delta^*} = 1196$. From equation (9) the amplitude of the disturbance, $|u_1|$, at the bump is predicted to be 4.90% of the free stream speed.

4. Experimental Results.

Figure 2 contains plots of the mean velocity profile across the boundary layer at two different streamwise locations. The locations are those labeled A and B in Figure 1 and the profiles are correspondingly labeled A and B in Figure 2. The solid lines are the Blasius profile for these locations while the * refers to the measured values. The normal distance between successive data points was approximately 0.1 mm with the data point closest to the boundary being at 0.2 mm from the surface. As can be seen, the measured mean profile was very close to Blasius. The three or four data points closest to the plate show a small but systematic deviation from the Blasius profile. We believe that this was a due to a wall interference effect with the hot wire. No corrections, near wall or otherwise, were made to the measured data after applying the calibrations factors for the wire.

The fact that the mean profile was Blasius was used to define the absolute distance of the hot wire from the plate at every (x-z) location. Before moving from one (x-z) location to another, the wire was moved out of the boundary layer. At the new location the wire was moved into the boundary layer until the mean velocity was that at $y = \delta^*$. This determined a datum from which other locations in the boundary layer were found. The

value of the velocity, as a fraction of the free-stream speed, at $y = \delta^*$ was taken to be that for a Blasius profile. The wire movement from one (x-z) location to another and finding the $y = \delta^*$ height was under computer control as part of the data collection program.

The main experimental measurements are those of the disturbance field. In all of these measurements the velocity field was sampled 128 times per second giving 64 data points per period for a 2 Hz driving frequency. At each location data was taken for either 32 seconds, providing 4096 data points, or 128 seconds, giving 16384 points. In either case the data set was divided into segments of 64 data points (either 64 or 256 segments) and averaged. The ensemble averaged waveforms were then Fourier analysed to obtain the first few coefficients. In all of the remaining figures we give plots of the intensity (amplitude) of the disturbance or intensity and phase. The phase is defined relative to the driver.

Profiles of the amplitude and phase of the 2 Hz fundamental across the boundary layer at both the A and B locations are shown in Figure 3. A is positioned about 105 boundary layer thickness downstream from the bump and B about 70 thicknesses. They were therefore expected to be in the far field of the oscillating bump. The intensity distributions at the two locations are very nearly the same. The peak intensity was about 0.2% and occurred about $\eta = 1.8$. Note that the intensity at A was slightly larger than that at B while the phase at both locations was essentially constant across the boundary layer. The disturbance field at the bump had a phase of $-\pi$ relative to the driver. Downstream of the bump, the phase was slightly larger than $-\pi$, with the phase at A being slightly larger than at B. The difference in phases seen in this figure, while small, was larger than any experimental error. The shape of the intensity and phase distributions are very different from those of Tollmien-Schlichting waves.

The effect of changing the amplitude of the driver motion on the disturbance field is shown in Figure 4. Three runs were made with different drive amplitudes and the intensity and phase profiles were measured at location B. The curves labeled B are the same results as those of Figure 3 with the standard driver amplitude of 0.12 mm ± 50%. For case C the driver amplitude was increased by $\sqrt{2}$ and for case D by 2 with respect to the standard driver amplitude. The intensity distribution for B, C divided by $\sqrt{2}$ and D divided by 2 are plotted in Figure 4. The phases are also plotted. It is clear that the intensity and phase curves are the same within the experimental run to run variation. Thus the flow disturbance in the far field of the oscillating bump was sufficiently small for the flow to be treated as a linear perturbation. This was also true of the first harmonic (4 Hz) disturbance field as shown in Figure 5. As stated above, even though the fluid velocity field is a linear function of the driver amplitude, the finite amplitude of the driver motion produces all harmonics. The first harmonic disturbance field, with the magnitude scaled by 1, 2 and 4 for driver amplitudes of 1, $\sqrt{2}$, and 2 respectively, has the same shape as the fundamental. Note that the intensity is much smaller in magnitude compared to the fundamental and that there is also more scatter than in the fundamental. We also measured the intensity and phase distributions of the second harmonic. These also have the same shapes but exhibited even more scatter.

A series of profiles through the boundary layer were measured along the line d-d shown in Figure 1. The purpose of these measurements was to examine the flow field in a region close to the bump, including the region upstream of the bump. Figure 6 shows intensity profiles in the boundary layer at intervals 5 mm along the line labeled d-d of Figure 1. The measurements were taken at y spacings twice those of the measurements shown in Figures 3 to 5 and so some detail is lost, particularly close to the plate. However, the general shape of the profiles was determined. First it should be noted that the diaphragm extended from x = 390 mm to x = 410 mm although the bump occupied only half of these in the region x = 395 mm to 405 mm. It can be seen that in this region there is a very large disturbance flow field extending well over half the boundary layer thickness. The profiles are quite different from those measured downstream at locations A and B. However, at distances greater than about one bump radius (10 mm) downstream the profiles are very similar to those at locations A and B. Upstream of the bump ($x < 390$ mm) there was a small disturbance which disappeared for $x \leq 360$ mm, which is more than one and one half bump diameters upstream. Directly above the source the intensity plots show a phase reversal indicated by the curves touching the vertical axes. Examination of the phase of the records at these locations confirmed this observation.

All of the results shown in Figures 2 through 6 are profiles of the disturbances normal to the plate at various streamwise locations. Additional measurements were made to determine the profiles in the spanwise (z) direction to determine the variation with streamwise (x) position. All of these measurements were made at the same position within the boundary layer, namely at a distance of one displacement thickness from the plate. At each location the appropriate y location was found by the procedure described above.

The results of a series of spanwise profiles at streamwise locations from x = 400 mm to x = 900 mm at x intervals of 25 mm are shown in Figures 7 and 8. These measurements spanned the region z = -25 mm to z = 25 mm in intervals of 1.0 mm. The region covered by these measurements is contained within the rectangle shown in Figure 1. Figure 7 shows the in phase component of the velocity and Figure 8 the out of phase component. The first of these profiles, that at x = 400 mm, crosses the center of the bump. At this location the fluid velocity is entirely in phase with the motion of the bump. The in phase component has roughly a Gaussian shape in z with a maximum of approximately 1.0% and the out of phase velocity component is zero. The maximum of the in phase component is not at x = 0 but at x = 1.5 mm. This could be due to either an error in the initial placement of the hot wire over the center of the bump or to a small misalignment of the driver rod with respect to the normal to the surface. The magnitude of the in phase component decreases with increasing x and side lobes also develop. In contrast, the magnitude of the out of phase component increases with increasing x. At x = 900 mm the magnitude of both the in and out of phase components is nearly the same and their spanwise distributions are almost identical.

A more detailed set of spanwise profiles are shown in Figures 9 and 10. These profiles were measured at three streamwise locations, x = 500 mm, 600 mm and 700 mm. These measurements spanned the region z = -40 mm to z = 40 mm in intervals of 0.5 mm

and all were made at $y = \delta^*$. These measurements were made along the lines labeled a - a, b - b and c - c of Figure 1. Figure 9 shows the in phase component of the velocity while Figure 10 shows the out of phase component. These more detailed results confirm those shown in Figures 7 and 8. There is a major difference between the in phase profiles at x = 500 mm as compared to the in phase profile in the vicinity of the bump. The unimodal, roughly Gaussian, profile at x = 400 mm has become, at x = 500 mm, a double peaked profile which is nearly symmetric about the centerline of the plate. This shape persists at both x = 600 mm and x = 700 mm with some minor modifications. The out of phase component is almost zero at x = 500 mm but grows slowly between x = 500 mm and x = 700 mm. At x = 700 mm the profile shape of the out of phase component is very similar to that of the in phase component.

Both Figures 9 and 10 have locations marked A and B, which mark the locations where the detailed profiles of the mean and disturbance velocities were made (Figures 2 to 5, inclusive). These x - z locations were chosen so as to be out of the near field of the bump. The x locations are about 70 and 105 boundary layer thicknesses downstream of the center of the bump. The z locations were chosen so as to maximize the intensity of the disturbance velocity. It is obvious that location A is closer to the centerline of the plate than is location B. The entire z profile is progressively shifted towards negative z at downstream x locations. This effect is also apparent in the results shown in Figures 7 and 8. It appears that the flow in the working section of the tunnel is not directed directly down the axis of the tunnel but is tilted at slight angle downwards. From this data we estimate that the tilt angle is about 1^o. Other experiments in the tunnel confirm the existence of the tilt and yield an estimate of about 1^o for the angle. We do not know the cause of this tilt. It could be due to a very small spanwise pressure gradient caused by differences in the thicknesses of the boundary layers on the working section floor and roof. We do not believe that this tilt had any major effect on the results of this experiment.

The spectrum of the disturbance velocity as a function of the cross stream mode number is shown in Figure 11 at the three x locations, x = 500, 600 and 700 mm, at which detailed spanwise profiles were measured. In this figure the symbols indicate the values obtained from the spectrum analysis and the continuous curve is a smooth interpolation obtained by calculating the spectrum at fractional wave numbers. The scale is such that the spanwise wavelength corresponding to a spanwise mode k is 80/k mm.

At x = 500 mm there is a large peak very close to k = 6, corresponding to a wavelength of 13.3 mm. The driver is 20 mm in diameter and is held rigidly at the edges so we infer that this component is the result of the driver motion. At x = 500 mm there is also a peak in the spectrum at k = 0 and another small peak at about k = 2 (wavelength about 40.0 mm). At x = 600 mm the peak at k = 0 has nearly vanished but that near k = 2 has grown to be almost as large as the peak at the primary, k = 6. By x = 700 mm the peak near k = 2 has become the dominant component in the spectrum. This effect is just barely visible in the data shown in Figures 9 and 10: there is a slight uniform increase in the measured values in the region z = ± 20 mm at x = 700 mm as compared to x = 500 mm. The peak at k = 6 decreases about 3% per 100 mm, but the peak near k = 2 has

increased by a factor of 8 between x = 500 mm and x = 700 mm. We attempted to examine the structure of the spanwise spectrum at other locations by calculating the spectrum of the data shown in Figures 7 and 8. However, the coarser spatial resolution (1 mm spacing versus 0.5 mm spacing) and the smaller range (± 25 mm versus ± 40 mm), resulted in such poor spectral resolution that downstream evolution of the components could not be observed.

The fact that the secondary peak appears very close to a mode number k = 2 (the peak of the smooth interpolation is at k = 2.25, a wavelength of 35.6 mm) while the primary peak appears at k = 6, suggests that the secondary peak is not a subharmonic of the primary. We do not know what mechanism is responsible for the appearance of the long wave length spectral peak.

5. Summary and Conclusions.

We have measured the disturbance velocity field in a boundary layer generated by a shallow oscillating bump on the surface of a flat plate. The bump oscillated at a very low frequency of 2 Hz, and thus the perturbation to the flow was quasistatic. The maximum height of the bump was about 4% of the local boundary thickness and induced a 5% fluctuating component in the flow just above the bump. The disturbance was entirely confined to the boundary layer. About 100 boundary layer thicknesses downstream of the bump the intensity had a maximum near $\eta = 2$ with a magnitude of about 0.2%. The spanwise profiles of the disturbance field changed dramatically from the near-field region of the bump to the far downstream region. The spanwise spectrum of the disturbance showed a primary peak consistent with the motion and geometry of the driver. This peak decreased by about 3% per 100 mm in x. In addition, a small secondary peak in the spectrum was apparent near the bump. This peak increased by a factor of 8 between x = 500 mm and x = 700 mm. The data show that the secondary peak is not at a wavenumber equal to one half that of the primary peak and so is not a subharmonic of the primary. We do not know what mechanism is causing the generation of the secondary peak.

At the time of these experiments we had some results from two-dimensional theories, but nothing from the three-dimensional case. It is unfortunate that experiments are more easily performed with three-dimensional excitation than two-dimensional ones, whereas the reverse is true for analytical or computational work. We will not report the results of the theoretical studies here because they are more appropriately linked to other experiments being carried out. The extension of the theories to cater for three-dimensional disturbances can be done, but requires some effort. It appears, however, that the predictions from current models will not reflect the observations made in the present series of measurements.

REFERENCES

P.W. Duck and O.R. Burggraf (1986) "Spectral solutions for three-dimension triple-deck flow over surface topography", *J Fluid Mech., 162, pp. 1-22.*

F.T. Smith (1982) "On the high Reynolds number theory of laminar flows", *IMA Journal of Applied Mathematics, 28, pp. 207-281.*

G.I. Taylor (1939) "Some recent developments in the study of turbulence", Proceedings of the Fifth International Congress for Applied Mechanics, J.P. Den Hartog and H. Peters, eds., John Wiley & Sons, Inc.

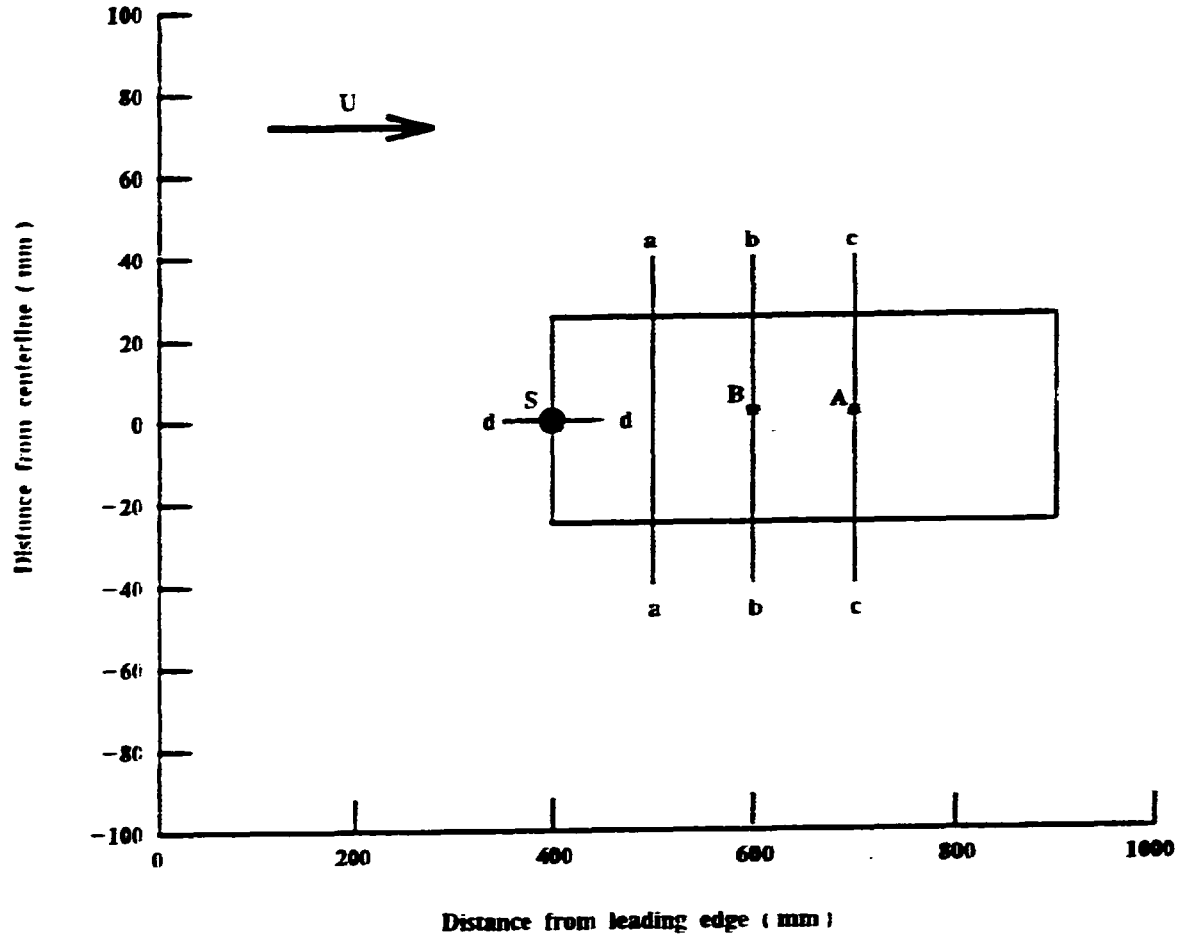

Figure 1. Sketch of the flat plate showing the location of the bump, which is denoted by S and is not drawn to scale, and locations where measurements were made.

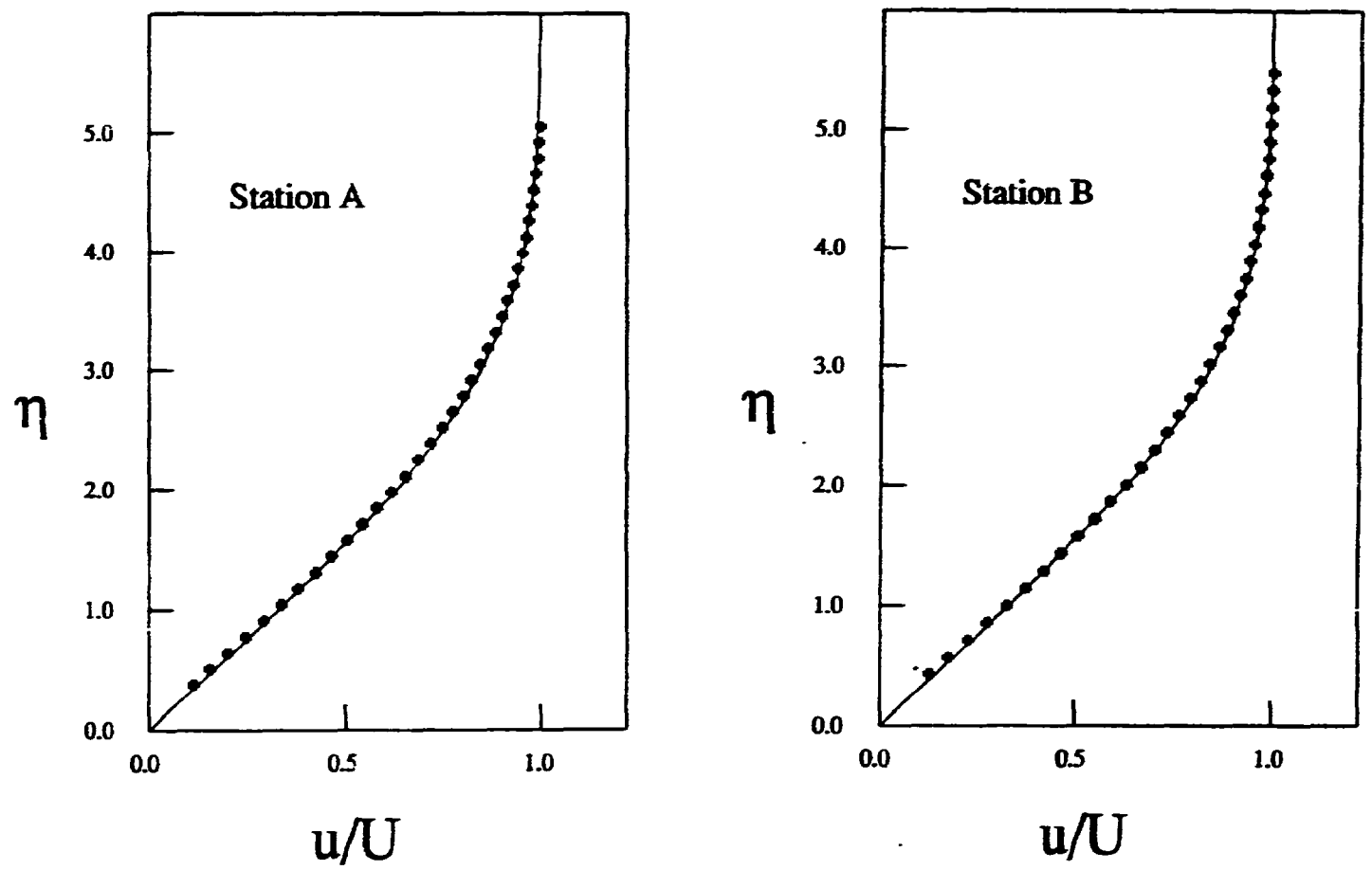

Figure 2. Profile of the mean velocity in the boundary layer at two locations. The locations are those labeled A and B in Figure 1. The profiles are correspondingly labeled A and B in this Figure. The points indicate the measured values and the solid lines are the calculated Blasius profile at these locations.

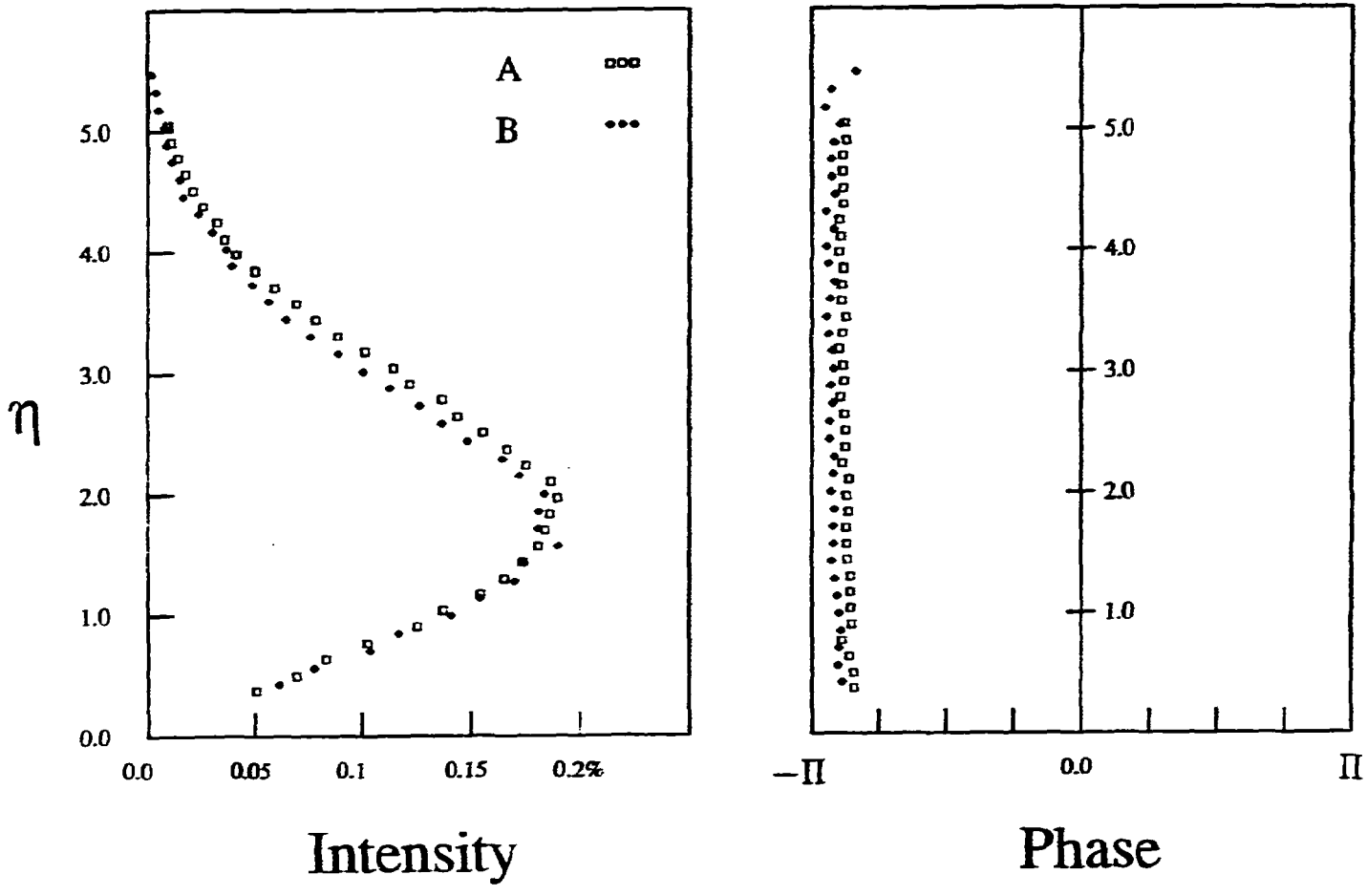

Figure 3. Intensity and phase profiles in the boundary layer of the disturbance field at the fundamental frequency of the driver. Measurements at the locations labeled A and B are shown.

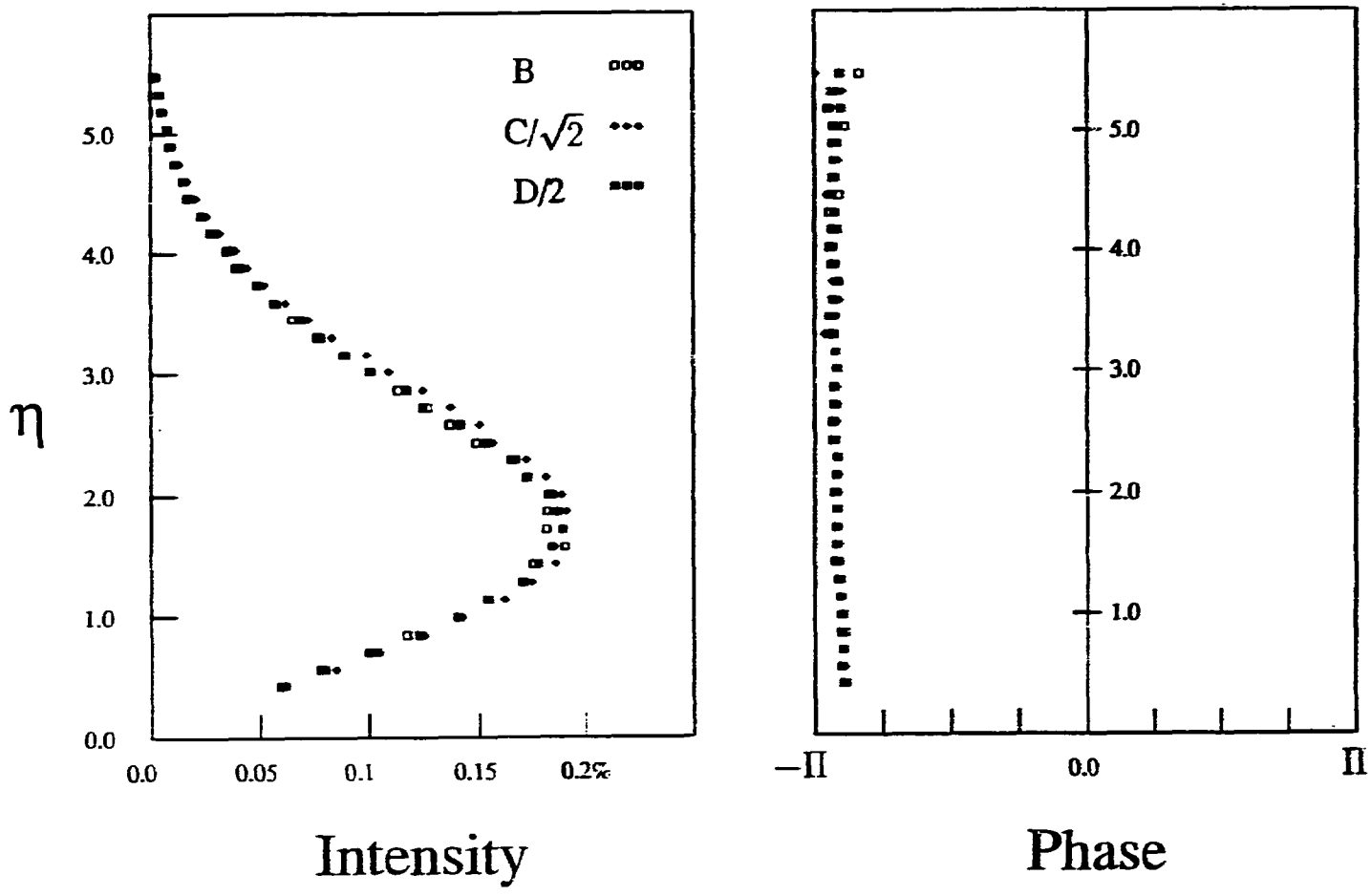

Figure 4. Intensity and phase profiles in the boundary layer of the disturbance field at the fundamental frequency of the driver. Measurements at location B are shown for three different amplitudes of the driver; the standard amplitude, $\sqrt{2}$ times, and 2 times the standard amplitude. The intensity profiles are scaled by 1, $\sqrt{2}$ and 2, respectively.

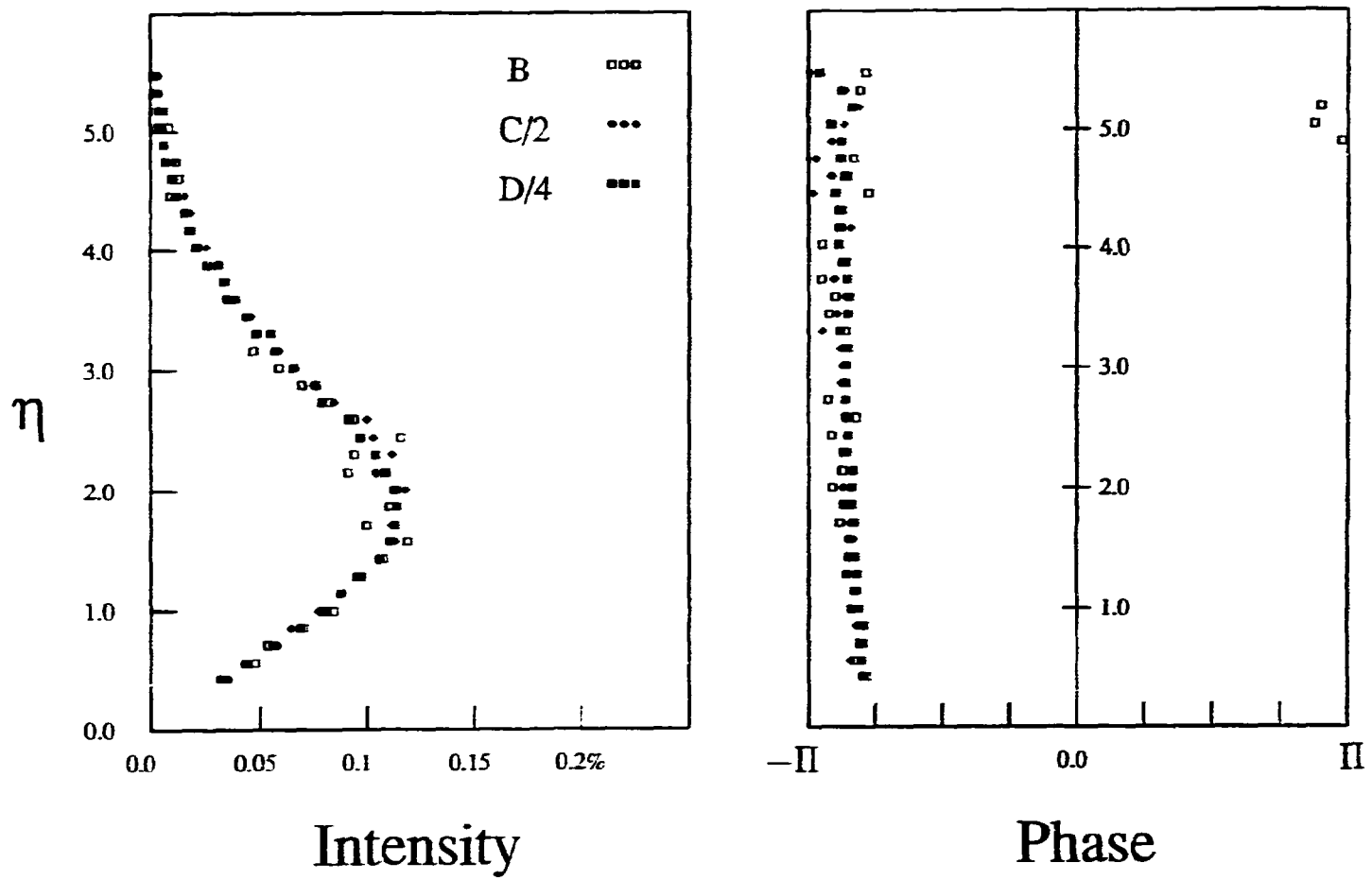

Figure 5. Intensity and phase profiles in the boundary layer of the disturbance field at the first harmonic frequency of the driver. Measurements at location B are shown for three different amplitudes of the driver; the standard amplitude, $\sqrt{2}$ times, and 2 times the standard amplitude. The intensity profiles are scaled by 1, 2 and 4, respectively.

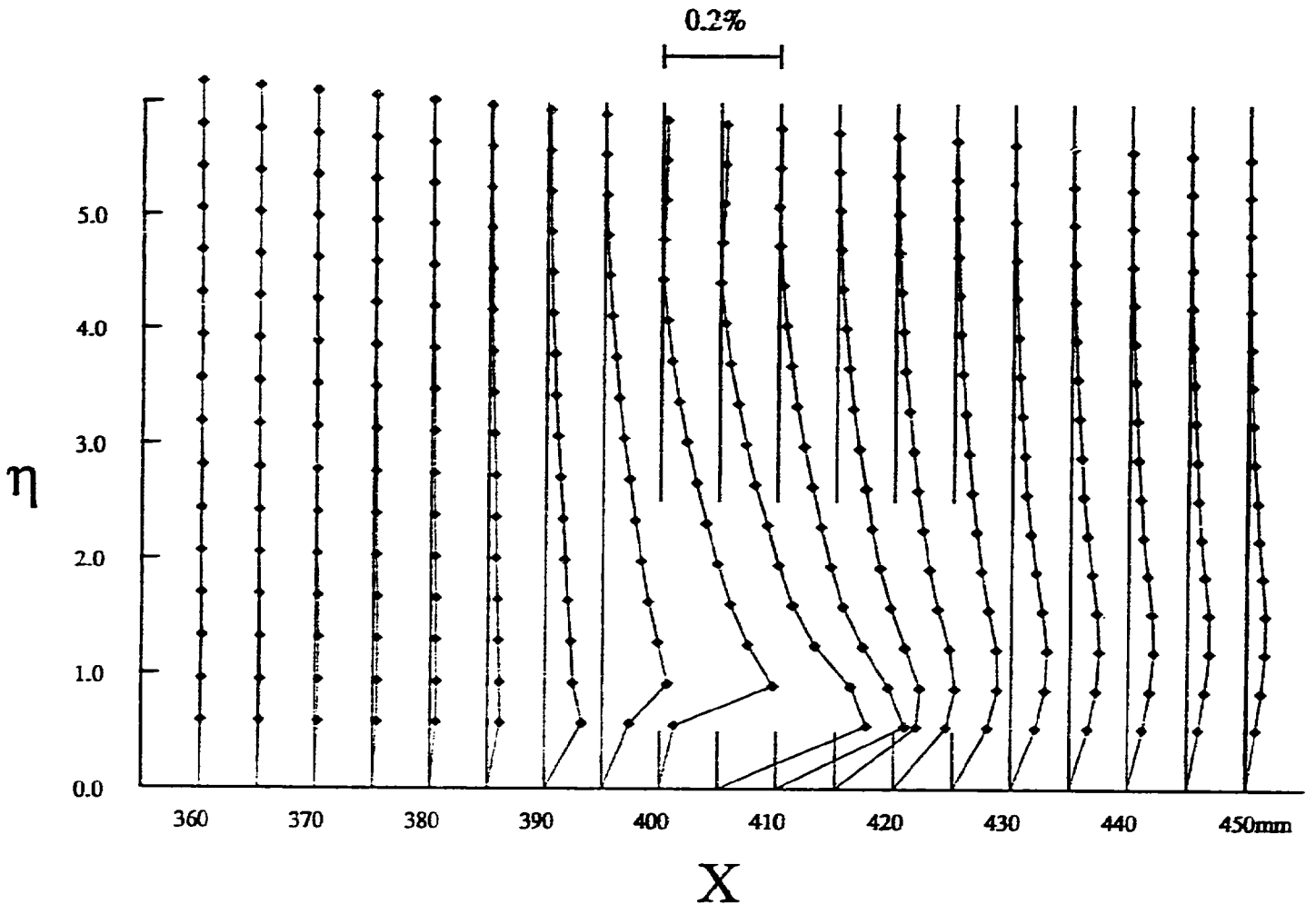

Figure 6. Intensity profiles of the disturbance in the boundary layer at intervals 5 mm along the line labeled d-d of Figure 1. The bump extends from x = 390 mm to x = 410 mm.

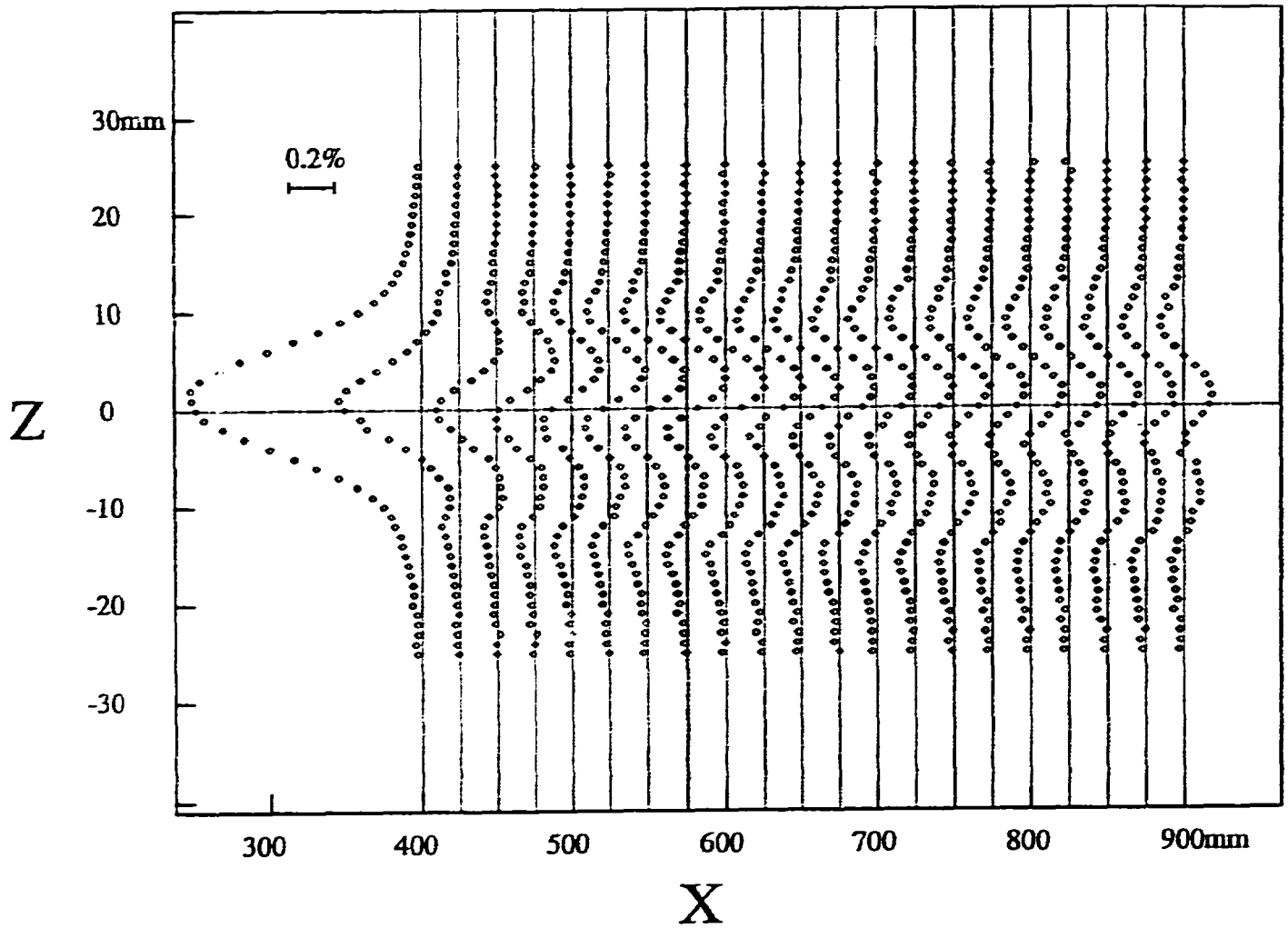

Figure 7. Spanwise intensity profiles of the in phase component of the disturbance at a height of $y = \delta^*$ and at streamwise locations from x = 400 mm to x = 900 mm at x intervals of 25 mm. The measurements spanned the region z = -25 mm to z = 25 mm in intervals of 1.0 mm. The region covered by these measurements is contained within the rectangle shown in Figure 1.

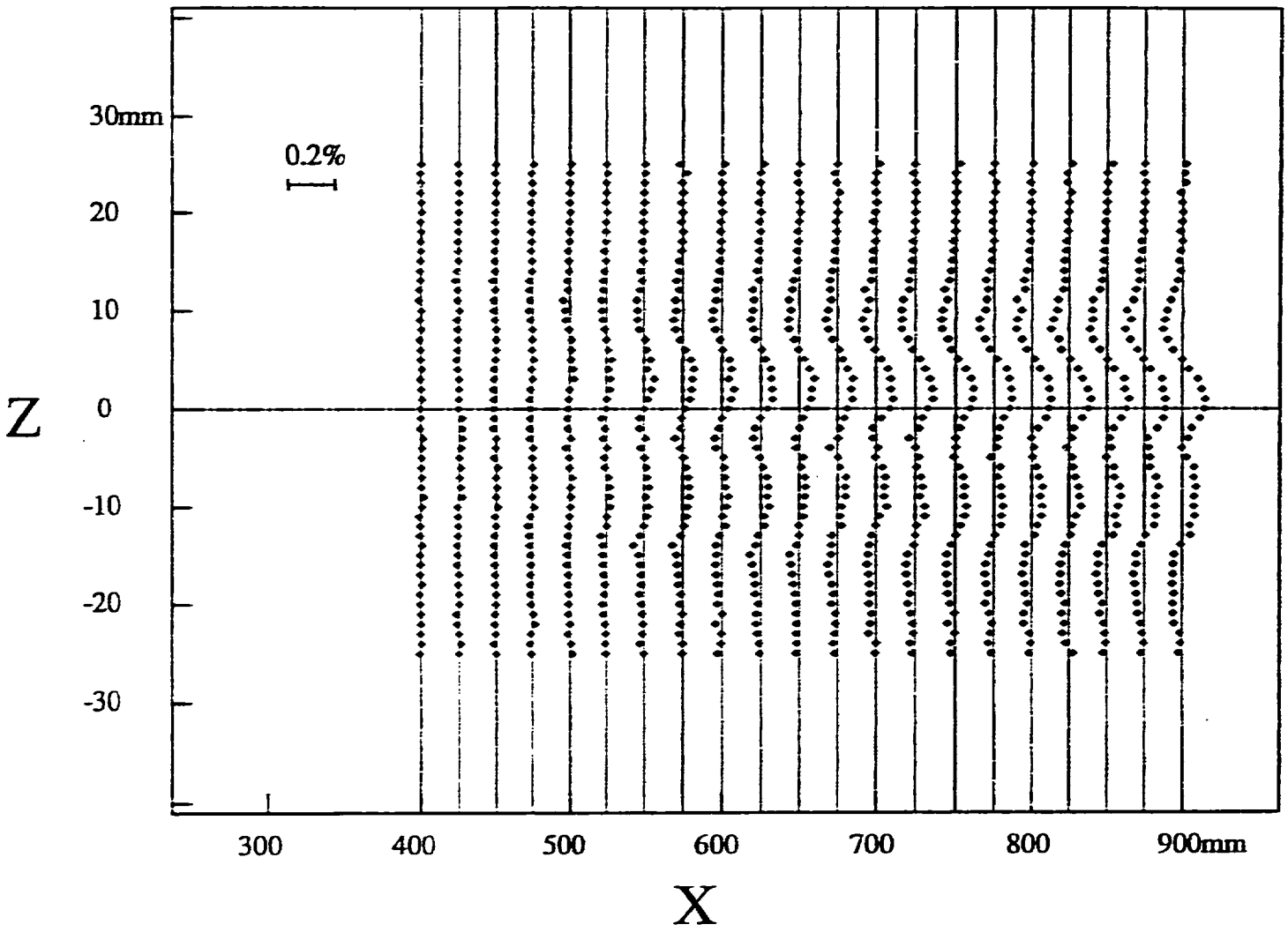

Figure 8. Spanwise intensity profiles of the out of phase component of the disturbance at a height of $y = \delta^*$ and at streamwise locations from x = 400 mm to x = 900 mm at x intervals of 25 mm. The measurements spanned the region z = -25 mm to z = 25 mm in intervals of 1.0 mm. The region covered by these measurements is contained within the rectangle shown in Figure 1.

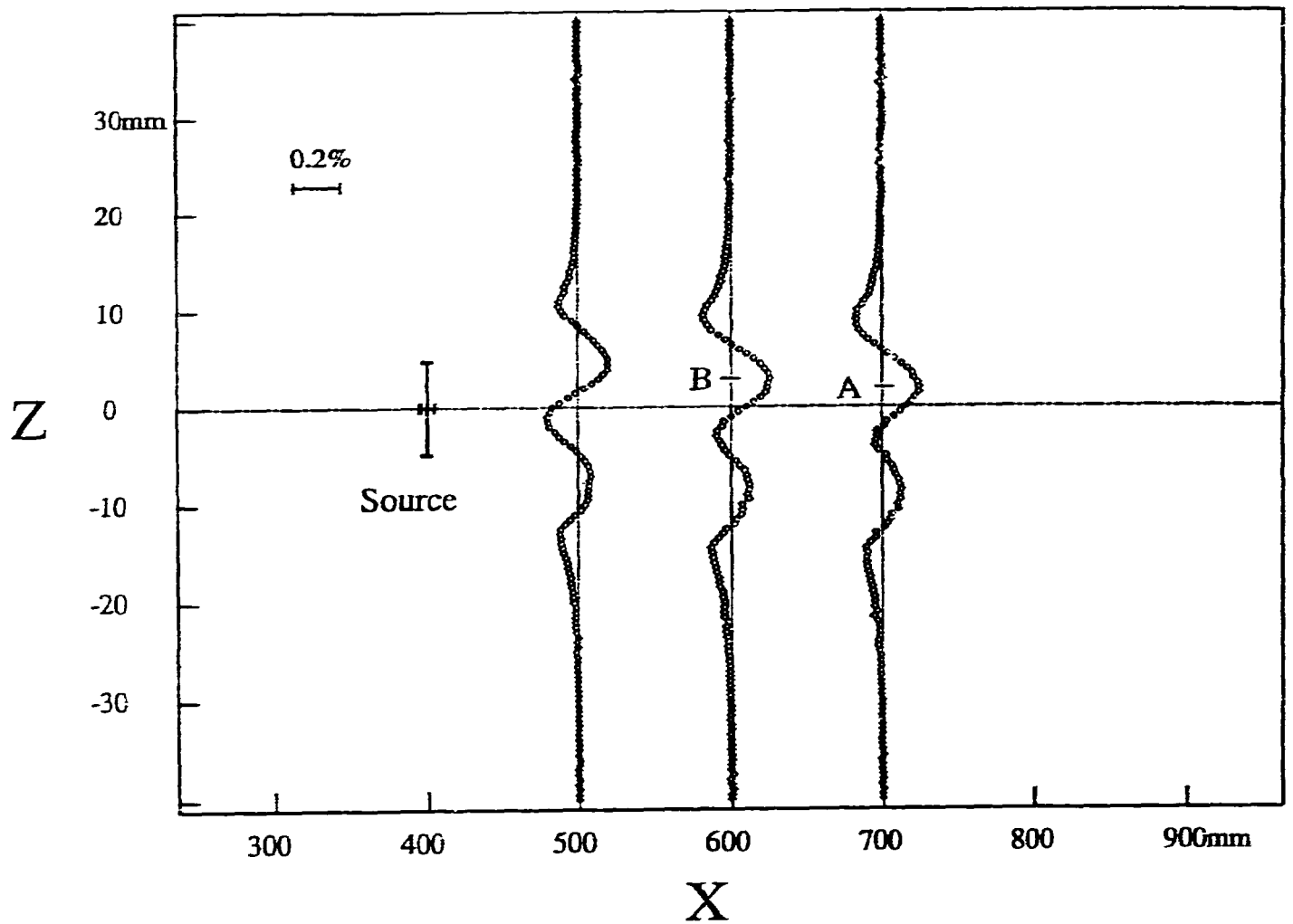

Figure 9. Spanwise intensity profiles of the in phase component of the disturbance at a height of $y = \delta^*$. These profiles were measured at three streamwise locations, x = 500 mm, 600 mm and 700 mm. These measurements spanned the region z = -40 mm to z = 40 mm in intervals of 0.5 mm. These measurements were made along the lines labeled a - a, b - b and c - c of Figure 1.

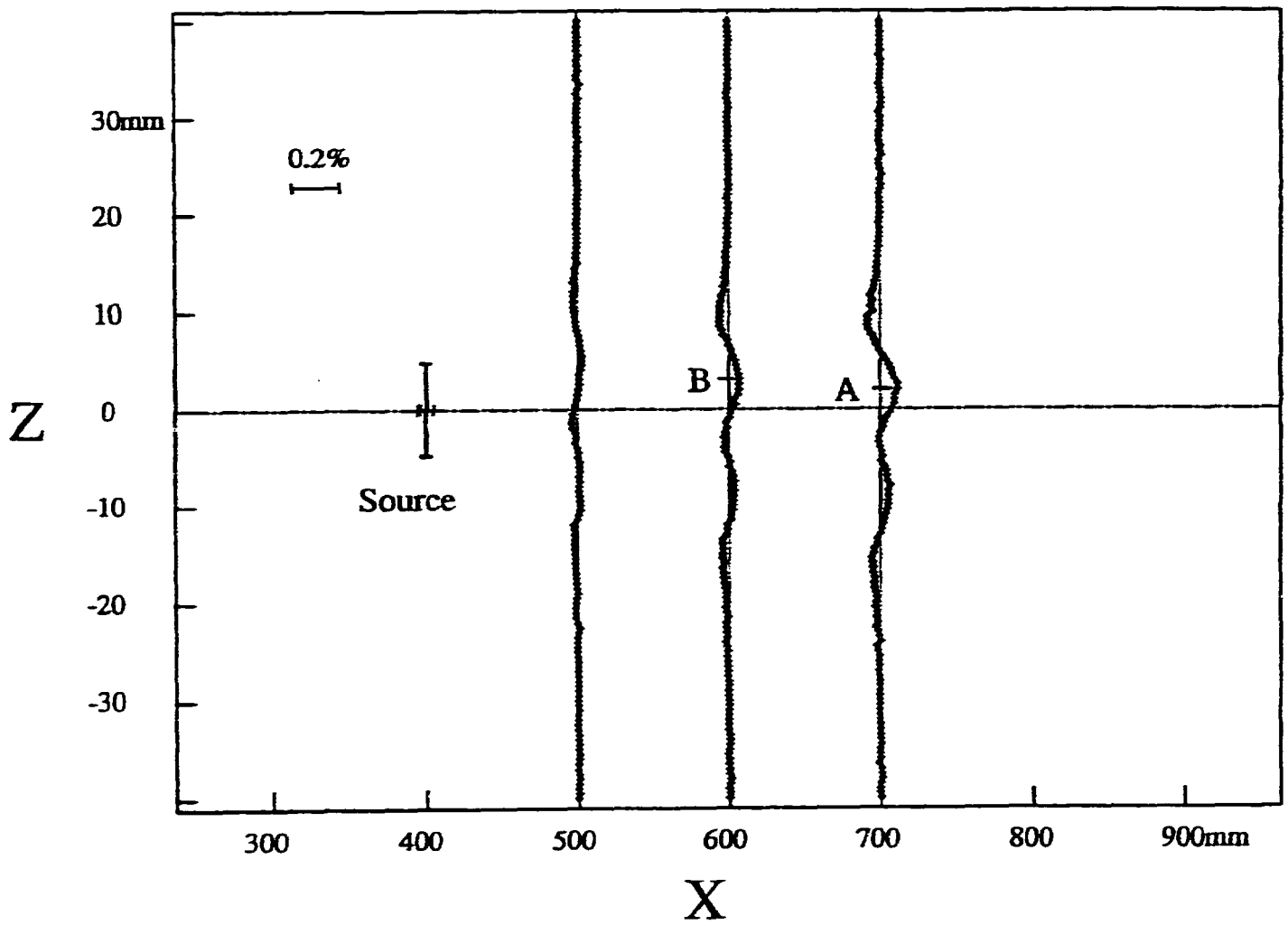

Figure 10. Spanwise intensity profiles of the out of phase component of the disturbance at a height of $y = \delta^*$. These profiles were measured at three streamwise locations, x = 500 mm, 600 mm and 700 mm. These measurements spanned the region z = -40 mm to z = 40 mm in intervals of 0.5 mm. These measurements were made along the lines labeled a - a, b - b and c - c of Figure 1.

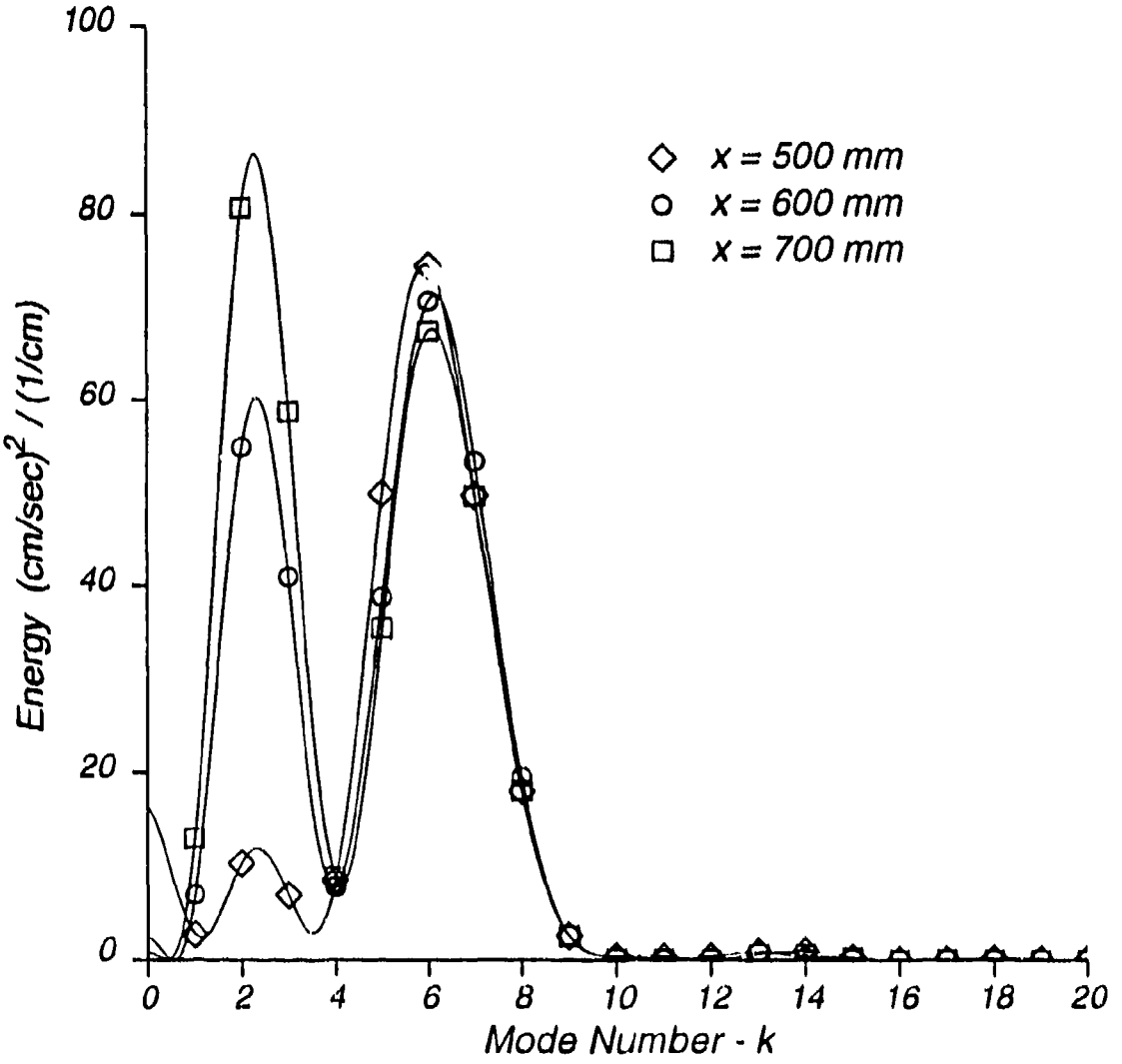

Figure 11. The spectrum of the spanwise intensity profiles component of the disturbance at a height of $y = \delta^*$. The spectra are for the three streamwise locations, x = 500 mm, 600 mm and 700 mm corresponding to the lines labeled a - a, b - b and c - c of Figure 1. The wavelength of a mode number k is given by 80/k mm.

REPORT DOCUMENTATION PAGE

Form Approved
OMB No 0704-0188

1. AGENCY USE ONLY *(Leave blank)*	2. REPORT DATE	3. REPORT TYPE AND DATES COVERED
	April 1994	Contractor Report

4. TITLE AND SUBTITLE
THE VELOCITY FIELD CREATED BY A SHALLOW BUMP IN A BOUNDARY LAYER

5. FUNDING NUMBERS
C NAS1-19480
WU 505-90-52-01

6. AUTHOR(S)
Michael Gaster
Chester E. Grosch
Thomas L. Jackson

7. PERFORMING ORGANIZATION NAME(S) AND ADDRESS(ES)
Institute for Computer Applications in Science
and Engineering
Mail Stop 132C, NASA Langley Research Center
Hampton, VA 23681-0001

8. PERFORMING ORGANIZATION REPORT NUMBER
ICASE Report No. 94-21

9. SPONSORING/MONITORING AGENCY NAME(S) AND ADDRESS(ES)
National Aeronautics and Space Administration
Langley Research Center
Hampton, VA 23681-0001

10. SPONSORING/MONITORING AGENCY REPORT NUMBER
NASA CR-194899
ICASE Report No. 94-21

11. SUPPLEMENTARY NOTES
Langley Technical Monitor: Michael F. Card
Final Report
Submitted to Physics of Fluids

12a. DISTRIBUTION/AVAILABILITY STATEMENT
Unclassified–Unlimited

Subject Category 34

12b. DISTRIBUTION CODE

13. ABSTRACT *(Maximum 200 words)*

We report the results of measurements of the disturbance velocity field generated in a boundary layer by a shallow three-dimensional bump oscillating at a very low frequency on the surface of a flat plate. Profiles of the mean velocity, the disturbance velocity at the fundamental frequency and at the first harmonic are presented. These profiles were measured both upstream and downstream of the oscillating bump. Measurements of the disturbance velocity were also made at various spanwise and downstream locations at a fixed distance from the boundary of one displacement thickness. Finally, the spanwise spectrum of the disturbances at three locations downstream of the bump are presented.

14. SUBJECT TERMS	15. NUMBER OF PAGES
Boundary layers, receptivity, experiments shallow bump	24
	16. PRICE CODE A03

17. SECURITY CLASSIFICATION OF REPORT	18. SECURITY CLASSIFICATION OF THIS PAGE	19. SECURITY CLASSIFICATION OF ABSTRACT	20. LIMITATION OF ABSTRACT
Unclassified	Unclassified		

NSN 7540-01-280-5500

Standard Form 298 (Rev. 2-89)
Prescribed by ANSI Std. Z39-18
298-102

☆U.S. GOVERNMENT PRINTING OFFICE: 1994 - 538-064/86150